

29th International Conference on Knowledge-Based and Intelligent Information & Engineering Systems (KES 2025)

# Location-Aware Deep Neural Network for Predicting Indoor 5G RSSI and CQI Using Drone-Based External RF Sensing

David HASON RUDD<sup>a,b</sup>, Cesar SANIN<sup>b</sup>, Koh Ming EN<sup>c</sup>, Xingyi GAO<sup>a</sup>, MD Rafiqul ISLAM<sup>d</sup>, Mehedi HASAN<sup>b</sup>, Xianzhi WANG<sup>a</sup>, Angela HUO<sup>a</sup>, Guandong XU<sup>a</sup>

<sup>a</sup>University of Technology Sydney, 15 Broadway Road, Ultimo, 2007, Australia

<sup>b</sup>Australian Institute of Higher Education, 545 Kent Street, SYDNEY NSW 2000, Australia

<sup>c</sup>Nanyang Technological University, 50 Nanyang Ave, 639798, Singapore

<sup>d</sup>Charles Darwin University, Ellengowan Dr, Casuarina NT 0810, Australia

---

## Abstract

Achieving reliable indoor 5G coverage in high-rise urban environments is challenging due to the significant signal attenuation of higher frequency bands through building materials and the intricate layouts of modern architecture. Traditionally, assessing in-building coverage to meet mobile network operators' standards requires conducting indoor walk tests, a method that is both costly and time-consuming. This study aims to develop a scalable and cost-effective method for predicting and visualizing in-building 5G coverage using externally collected radio frequency (RF) data. We propose a methodology that employs AIoT-enabled drones equipped with cellular network scanners to gather key signal metrics, such as Received Signal Strength Indicator (RSSI) and Channel Quality Indicator (CQI), from the dominant 5G macrocell outside the building. The proposed Location-Aware Deep Neural Network (LA-DNN) integrates external radio frequency (RF) measurements with spatial coordinates, free-space path loss models, and material-specific attenuation factors to predict indoor RSSI and CQI. The model demonstrates robust predictive performance, achieving an  $R^2$  of 0.9567 with a root mean squared error (RMSE) of 8.75 dBm for RSSI, and an  $R^2$  of 0.9713 with an RMSE of 2.08 for CQI, validated against indoor walk-test data. Additionally, three-dimensional (3D) heatmaps are generated to visualize predicted coverage across building floors, facilitating the identification of coverage gaps and RF null zones. By minimizing the need for indoor measurements during initial in-building coverage assessments, the proposed framework significantly enhances the efficiency of site survey teams before implementing In-Building Coverage (IBC) systems.

© 2025 The Authors. Published by Elsevier B.V.

This is an open access article under the CC BY-NC-ND license (<https://creativecommons.org/licenses/by-nc-nd/4.0>)

Peer-review under responsibility of the scientific committee of the KES International.

**Keywords:** 5G mobile networks; In-building coverage; Drone-based RF sensing; Indoor coverage prediction; Deep learning; 3D indoor coverage visualization

---

URL: <https://davidhason.com> ()

\* Corresponding author

E-mail address: david.hasonrudd@uts.edu.au

## 1. Introduction

With 80% of mobile data traffic occurring indoors [1], ensuring reliable 5G in-building coverage (IBC) in high-rise urban settings is challenging due to signal attenuation (20–45 dB) through modern building materials [2, 3]. Traditional methods like indoor walk tests are costly and time-consuming [4, 5]. This study proposes an AIoT-enabled drone-based methodology to predict indoor RSSI and CQI using external RF data, eliminating the need for indoor measurements. A Location-Aware Deep Neural Network (LA-DNN) integrates drone-collected RF data with spatial and structural features [6, 7], while 3D heatmaps visualize predicted coverage [8]. This study significantly advances in-building 5G coverage assessment and optimization, offering a scalable framework for commercial IBC deployment. Key contributions include:

- A novel data-driven methodology for in-building 5G coverage prediction that uniquely leverages drone-collected external RF data, building structural characteristics (geometry and material properties), and advanced interpolation techniques, thereby eliminating the dependency on prior indoor walk test for initial IBC assessment.
- Development of an LA-DNN model which incorporates spatial coordinates, external RF measurements, and building characteristics, significantly improving prediction accuracy.
- Introduction of a 3D visualization tool for identifying coverage gaps.

## 2. Related Work

Significant advancements have recently enhanced cellular network coverage through drone and AIoT-driven solutions, integrating artificial intelligence (AI) with Internet of Things (IoT) technologies using drones equipped with RF scanners to address network coverage challenges. Employing drones as mobile base stations (drone-BSs) offers an efficient solution for targeted coverage in urban high-rise areas, though optimal placement remains challenging; Ouamri et al. (2022) [9] proposed a metaheuristic algorithm to optimize drone-BS deployment in 5G networks, improving coverage and capacity. Traditional signal quality assessments often rely on labor-intensive walk tests, but alternative ML approaches reduce human effort. Yuliana et al. (2024) [11] explored ML models like random forest and CNN for external 5G coverage prediction, identifying random forest as the top performer with a new feature on antenna distances. Davies, Grout, and Picking [12] developed a model for Wi-Fi coverage using Friis Transmission [13], noting challenges in manual data collection during building construction. Behjati et al. (2022) [15] used ML to predict RSRP and RSRQ from drone-collected external RF data, reducing operational costs for aerial communications. Dhekne et al. (2017) [19] highlighted drones' role in expanding coverage in high-density areas, emphasizing rapid deployment. Raj et al. (2021) [26] predicted indoor RSSI using ML models but noted scalability issues due to reliance on indoor measurements, underscoring the need for external data-driven methods like our drone-based approach. Despite such progress in drone-based solutions, most approaches focus on outdoor coverage optimization or require labor-intensive indoor walk-test surveys, with few studies exploring macrocell signal data for indoor 5G coverage prediction via ML—a method more feasible than collecting indoor RF data given building complexity. This study bridges these gaps by integrating drone-based RF scanning with ML to generate high-resolution indoor 3D coverage heatmaps, facilitating precise assessment and visualization of dominant cell coverage while offering significant cost savings over traditional methods.

## 3. Methodology

This section outlines a methodology for predicting indoor 5G coverage in high-rise buildings using drones and machine learning (ML).

### 3.1. Datasets, data acquisition and preprocessing techniques

We created four distinct datasets for this project as follows. A drone equipped with TEMS Pocket™ and G-MoN collected 5G RSSI and CQI data around a Sydney high-rise, sampling every 3 s at 4 km/h.

- External RF (out-building) dataset: Collected via drone, capturing dominant macrocell signal parameters (e.g., RSSI, CQI) around the building using circular flight paths at each floor.
- Internal RF (in-building) dataset: Gathered from walk-tests across 10 floors, used as a validation benchmark.
- Building characteristics dataset: Includes structural details (e.g., wall materials, average wall count between exterior and core, distance to core).

The data preprocessing involved data normalization and spatial feature integration, where features such as RSSI, RSRP, RSRQ, CQI, and SNR were normalized, and spatial data including altitude, speed, and coordinates enriched positional context. Data augmentation was performed by simulating intermediate points between external measurements using RF propagation interpolation. For feature selection, 18 key features were chosen from an initial set of 43, encompassing 5G metrics (RSSI, RSRP, CQI, SNR, RSRQ) and spatial attributes (distance, coordinates, wall count). This per-floor data acquisition strategy, combined with the recording of precise altitude data, inherently allows the framework to accommodate buildings with variable floor heights.

### 3.2. Baseline model framework details

The baseline model leverages external radio frequency (RF) data, augmented with key in-building features, to predict indoor 5G coverage. These features include core RSSI ( $P_{rc}$ ), free-space path loss ( $PL_{\text{free space}}$ ), and building penetration loss ( $PL_{\text{bldg loss}}$ ). Two approaches were implemented: a Gradient Boosting Tree (GBT) with 150 trees, a maximum depth of 7, and a learning rate of 0.100, and a Deep Neural Network (DNN) with two hidden layers of 50 neurons each (ReLU activation) and a linear output layer. These models provide a benchmark for evaluating advanced methods. The baseline model comprises the following steps:

1. **External RF Data Collection:** Drones equipped with RF scanners collect signal parameters (RSSI, RSRQ, SNR, RSRP, CQI) from the dominant macrocell around the building perimeter.
2. **Core RSSI Calculation:** The received power at the building core ( $P_{rc}$ ) is calculated using Equation (1), where  $P_{rd}$  is the RSSI at the drone's location,  $PL_{\text{free space}}$  is the free-space path loss, and  $PL_{\text{bldg loss}}$  is the building penetration loss:

$$P_{rc} = P_{rd} - (PL_{\text{free space}} + PL_{\text{bldg loss}}) \quad (1)$$

3. **Feature Enrichment:** Three features are derived from the in-building dataset to enhance the model's ability to predict indoor signal parameters, focusing on RSSI and CQI:
  - Free-space path loss ( $PL_{\text{free space}}$ ) is computed as per Equation (2), where  $d$  is the distance,  $f$  is the frequency, and  $\lambda$  is the wavelength:

$$PL_{\text{free space}} = 20 \log_{10}(d) + 20 \log_{10}(f) + 20 \log_{10}\left(\frac{4\pi}{\lambda}\right) \quad (2)$$

- Building penetration loss ( $PL_{\text{bldg loss}}$ ) is determined using Equation (3), where  $\alpha_i$  and  $d_i$  represent the attenuation coefficient and thickness of material  $i$ , respectively:

$$PL_{\text{bldg loss}} = \sum_i (\alpha_i \times d_i) \quad (3)$$

- Core RSSI ( $P_{rc}$ ) is computed using Equation (1) with the above losses.

### 3.3. Calibration techniques for accurate data point alignment

Accurate positioning of data points is essential for training location-aware machine learning models, and Figure 1 highlights significant GPS inaccuracies in the raw data, especially in the in-building dataset, due to poor signal reception and obstructions. To address this, a data point calibration tool was developed to align recorded data with the actual paths taken during network scanning by having users annotate the walk-test path for in-building data and the drone's flight path for external data on corresponding building floor plans, algorithmically repositioning the data points equidistantly along these annotated paths to ensure spatial consistency, and using a turbo colormap to represent key signal metrics (RSSI and CQI) for verification of data alignment. This calibration process enhances positional accuracy, reduces errors, and improves the reliability of model training for indoor building coverage (IBC) prediction.

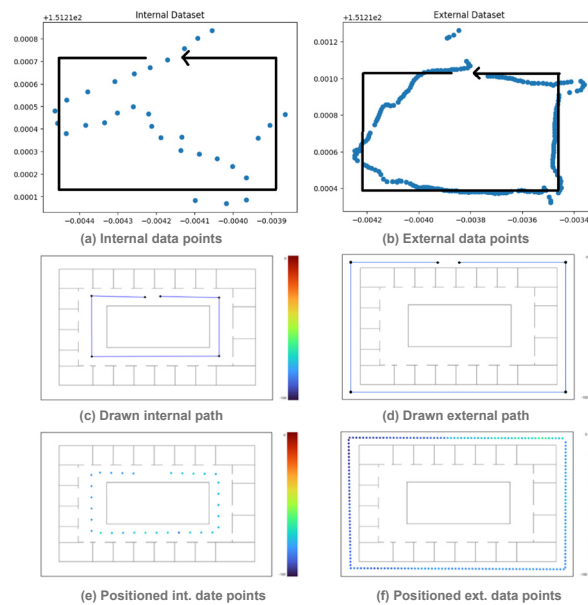


Fig. 1. Data point location discrepancies. (a) In-building and (b) external RF data points; (c) and (d) users generated paths on uploaded building floorplans for (a) and (b), respectively; and (e) and (f) data points positioned equidistantly along the user path for (a) and (b) respectively

## 4. Location-aware deep neural network with interpolation

The baseline model predicts indoor coverage by estimating signal attenuation based on free-space path loss and building material loss from the drone to the building core. However, it fails to account for detailed interior factors such as wall placement, wall materials, and the number of walls between points, all of which significantly impact signal propagation. By relying on averaged path loss values and lacking advanced interpolation techniques, the baseline simplifies coverage estimation and struggles to visualize predictions in a 3D map effectively. This approach proves inadequate for complex building layouts with multiple rooms or barriers. To overcome these limitations, we introduce an advanced model that incorporates interior design elements, improving in-building coverage (IBC) prediction accuracy for intricate environments.

Our methodology utilizes drone-collected external RF data alongside detailed floor plans, processed through a Location-Aware Deep Neural Network (LA-DNN) with K-Nearest Neighbors (KNN)-based interpolation. This approach integrates spatial coordinates, free-space path loss, and material-specific attenuation to predict indoor Received Signal Strength Indicator (RSSI) and Channel Quality Indicator (CQI). The process involves data augmentation, feature engineering, model training, and 3D heatmap visualization. This method enhances prediction precision by incorporating proximity-based interpolation and wall-induced attenuation, outperforming the baseline model. The following pseudocode encapsulates this workflow:

**Algorithm 1** LA-DNN with Interpolation

- 1: **Input:** External RF data points, internal points, floor plans, building features
- 2: **Output:** Predicted indoor RSSI and CQI, 3D heatmaps
- 3: **Step 1: Data Augmentation**
- 4: Fit KNN model to external RF data points
- 5: Generate synthetic samples using  $k$  nearest neighbors and wall counts
- 6: **Step 2: Feature Engineering**
- 7: Combine spatial coordinates, path loss, and material attenuation
- 8: **Step 3: Model Training**
- 9: Train LA-DNN with augmented dataset (layers: 1024, 512, 256)
- 10: **Step 4: Prediction and Visualization**
- 11: Predict RSSI and CQI for internal points
- 12: Generate 3D heatmaps for visualization

#### 4.1. Number of wall detection

We applied image processing techniques to floor plans, as shown in Figure 2, to assess wall-induced signal attenuation by first preprocessing the images through conversion to grayscale, applying Otsu's method [23] for thresholding, and using binary thresholding to enhance contrast, then utilizing Canny edge detection [24] to accurately delineate wall boundaries, and finally employing the probabilistic Hough transform [25] to detect and map wall lines, which enables precise calculation of wall counts along signal paths critical for accurate attenuation estimation. Signal strength prediction accounts for wall attenuation using the equation:

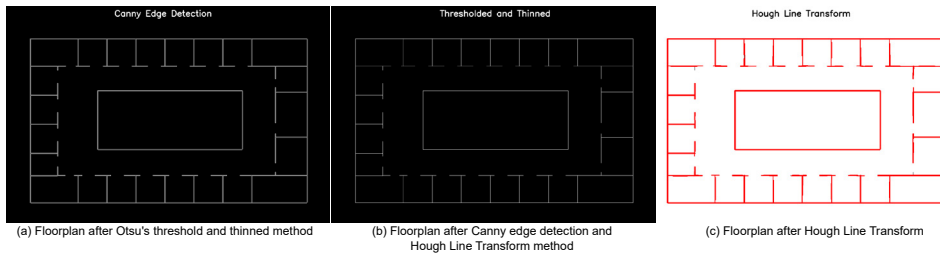


Fig. 2. Visualization of wall detection stages in the floorplan: (a) Floorplan after preprocessing using Otsu's method enhances image contrast by thresholding, (b) Application of Canny Edge Detection to identify precise wall boundaries, and (c) Wall detection and line mapping using the Probabilistic Hough Line Transform to calculate the number of walls impacting signal paths.

$$\hat{y} = p_0 + \frac{1}{k} \sum_{i=0}^k n^{m_i} y_i \quad (4)$$

where  $p_0$  represents the base signal value,  $k$  is the number of nearest neighbors,  $m_i$  is the wall count between the external RF point  $y_i$  and the target, and  $n$  is the damping factor. Hyperparameter optimization via grid search yielded optimal values: for RSSI,  $p_0 = -20$ ,  $n = 0.9$ ,  $k = 10$ ; for CQI,  $p_0 = 2$ ,  $n = 0.97$ ,  $k = 10$ . The LA-DNN incorporates features such as RSSI, CQI, Reference Signal Received Power (RSRP), Reference Signal Received Quality (RSRQ), Signal-to-Noise Ratio (SNR), and wall counts, derived from six KNN-selected external RF points per internal location. Building-specific attributes, including attenuation coefficients, dimensions, and wall types, further improve the model's adaptability to diverse structures.

#### 4.2. Data augmentation using $K$ -nearest neighbors

Given the limited dataset size per building level, which increases overfitting risks, we implemented KNN-based data augmentation to enrich the training data. This technique generates synthetic samples by integrating

external RF data with wall counts. In this study, we selected six neighbors and generated five synthetic points per internal point, resulting in 880 training samples and 176 test samples. This augmentation preserves spatial and structural relationships, enhancing model robustness and generalization. The process is detailed in the pseudo code below:

---

**Algorithm 2** Data Augmentation with KNN

---

```

1: Input: external_points, num_neighbors, num_dp
2: Output: Augmented training dataset
3: Fit KNN model with  $k = \text{num\_neighbors} \times \text{num\_dp}$ 
4: for each internal point do
5:   Identify  $k$ -nearest external points
6:   for num_dp iterations do
7:     Randomly select num_neighbors neighbors (excluding the closest)
8:     Calculate wall count to the internal point
9:     Combine RF features with wall count data
10:    Append to augmented dataset
11:   end for
12: end for

```

---

## 5. Evaluation metrics for interpolation accuracy

Accuracy was evaluated using two methods. The first method, known as Root Mean Square Error (RMSE) (5), quantifies prediction error as the square root of the average squared difference between actual ( $y$ ) and predicted ( $\hat{y}$ ) values:

$$\text{RMSE}(y, \hat{y}) = \sqrt{\frac{1}{N} \sum_{i=0}^{N-1} (y_i - \hat{y}_i)^2}, \quad (5)$$

where  $N$  represents the number of data points, and smaller RMSE values signify higher accuracy. The second method, referred to as Thresholding, deems predictions accurate if they fall within 10 dBm for RSSI and 3 units for CQI, evaluating the model's practical reliability within operational limits.

### 5.1. Deep neural network architecture for IBC prediction

The proposed Multilayer Perceptron (MLP) model predicts indoor RSSI and CQI values using a deep neural network architecture. The model comprises three hidden layers with 1024, 512, and 256 neurons, respectively, each followed by a Rectified Linear Unit (ReLU) activation function to introduce non-linearity. To mitigate overfitting, a dropout rate of 10% is applied after each hidden layer. The output layer employs a linear activation function, suitable for regression tasks. Hyperparameter optimization, conducted via grid search, identified an optimal learning rate of 0.001 and a weight decay of  $5 \times 10^{-6}$ . These settings effectively minimize the MSE loss, ensuring accurate predictions. The architecture balances simplicity and depth, providing scalability and high predictive accuracy for IBC applications.

### 5.2. Proposed IBC 3D heatmap visualization

We propose a tool to generate 3D heatmaps for 5G signal coverage within indoor environments, enhancing signal propagation analysis. Users can upload simulated in-building coverage datasets obtained from the proposed interpolation step, along with relevant floor plans and drone paths for each building level. Figure 3 shows that the server processes this data to predict signal coverage values, including Received Signal Strength Indicator (RSSI) and Channel Quality Indicator (CQI), ultimately producing 3D heatmaps through

interpolation. The simulated in-building dataset is uploaded in a manner that aligns with the training datasets. The server processes the in-building data by grouping it according to altitude, which allows identifying distinct building levels. The user is then prompted to upload the building floor plans and annotate the drone paths for each floor as part of the calibration process. These calibrated data point coordinates are updated in the simulated in-building datasets, and then the updated dataset is prepared for interpolation. The proposed

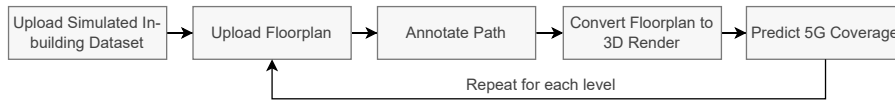


Fig. 3. Workflow for the proposed IBC 3D model

3D rendering tool predicts RSSI and CQI for each floor across a grid of evenly spaced points. Users can adjust the grid resolution, trading off between inference accuracy and processing speed. Building floor plans are transformed into 3D models through a pipeline that starts with line detection to identify walls within the 2D images, as discussed in Section 4.1. A 3D scene is constructed using Python Blender by extruding the walls along the Z-axis to a specified thickness. Height for each floor is inferred by evaluating altitude differences between adjacent levels. The walls are merged into a single object and exported in GLTF format for further processing. PyVista [22] is utilized to color the 3D walls with reference to interpolated RSSI and CQI values, centering the floor plans around the origin to ensure consistent alignment. This tool maps the interpolated values to the nearest walls through a nearest-neighbor strategy, producing a highly accurate representation of signal propagation. The final 3D render is visualized in a web application via the Three.js APIs, enabling dynamic exploration of the heatmaps. The proposed 3D rendering prototype provides a scalable and user-friendly solution for visualizing in-building coverage (IBC), facilitating network assessment and optimization performance for complex high-rise environments.

Figure 4 shows the workflow framework for the proposed Location-Aware Deep Neural Network (LA-DNN). The sequential stages include input data collection, preprocessing, feature engineering, model training, interpolation for making predictions, and 3D visualization for RSSI and CQI distributions within the building.

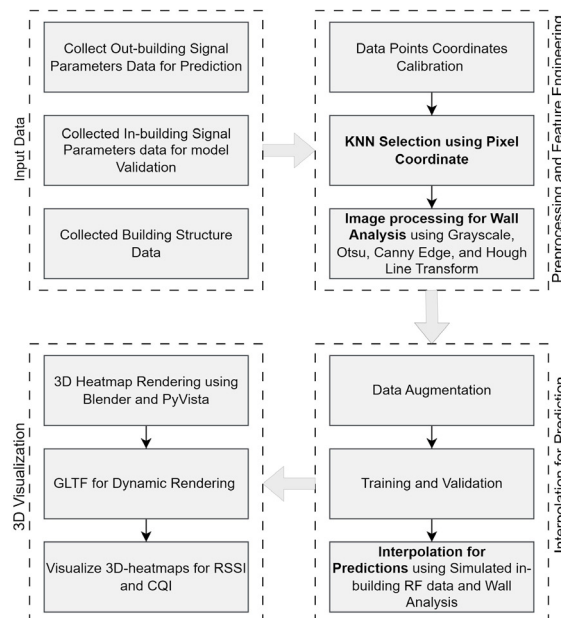


Fig. 4. Workflow of the Proposed LA-DNN Model for Predicting Indoor 5G Coverage

To clarify the 3D visualization process, the following pseudo code outlines the key steps:



**Algorithm 3** 3D Heatmap Visualization

- 1: **Input:** Floor plans, calibrated dataset, predicted RSSI/CQI
- 2: **Output:** Interactive 3D heatmap
- 3: **Step 1: Floor Plan Conversion**
- 4: Detect walls using line detection (Section 4.1)
- 5: Extrude walls in 3D using Blender
- 6: **Step 2: Grid Prediction**
- 7: Generate grid points for each floor
- 8: Predict RSSI/CQI at grid points
- 9: **Step 3: Coloring and Rendering**
- 10: Color walls using PyVista and nearest-neighbor interpolation
- 11: Export to GLTF and visualize with Three.js

**6. Results***6.1. Baseline model results*

The preprocessed dataset was split into 80% training and 20% test sets, with samples selected within floors. Figure 5 shows strong predictive accuracy for the Gradient Boosting Tree (GBT) model, with scatter plots and histograms indicating close alignment between predicted and actual RSSI and CQI values along the 45° line. However, deviations and a bimodal distribution suggest potential biases, indicating the need for further optimization. In comparing GBT and DNN, GBT outperformed with an RMSE of 1.373 vs. 3.335 for RSSI. Despite GBT's slightly better metrics, it lacks the LA-DNN's robust interpolation and adaptability to complex indoor environments, making LA-DNN more suitable for real-world deployment.

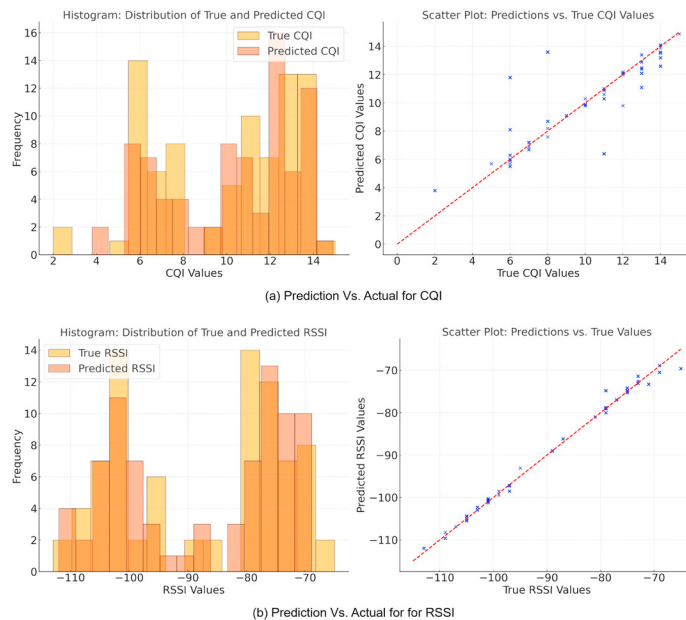


Fig. 5. Predictive accuracy and generalization for the baseline GBT model

*6.2. Proposed advanced model results*

The proposed advanced model was trained over 100 epochs, utilizing early stopping to mitigate overfitting. The model achieved impressive accuracy and RMSE = 95.671% and 8.7485 for RSSI; and 97.131% and 2.0757 for CQI; considerably improving upon the baseline methods. Figure 6 shows predicted distributions



closely align with actual distributions, highlighting the model's ability to effectively generalize. The results emphasize the superior performance of the proposed advanced model in accurately predicting IBC metrics, particularly for RSSI compared to CQI. This difference arises from the CQI signal parameters having significantly more inherent variability, which is not handled as well by the baseline model.

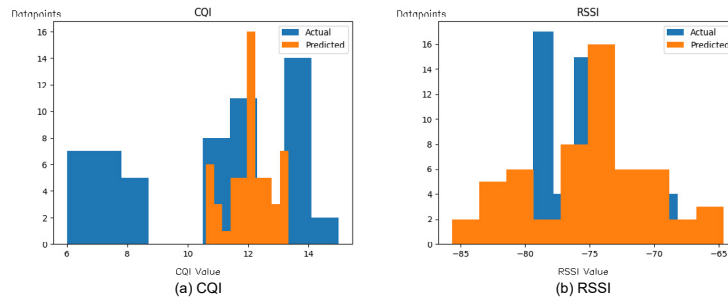


Fig. 6. Proposed advanced model (a) CQI and (b) RSSI prediction outcomes

### 6.3. Interactive 3D mapping for RSSI and CQI

Figure 7 shows 3D visualizations for RSSI and CQI predictions across several levels within the building from the proposed advanced model. These 3D heatmaps effectively highlight spatial variations in signal strength and quality, enabling precise prediction of coverage gaps and RF null zones within buildings. Thus, the proposed framework, leveraging external RF data collected by drone and integrating predictive modeling results with building structural data, provides an intuitive and actionable representation for IBC.

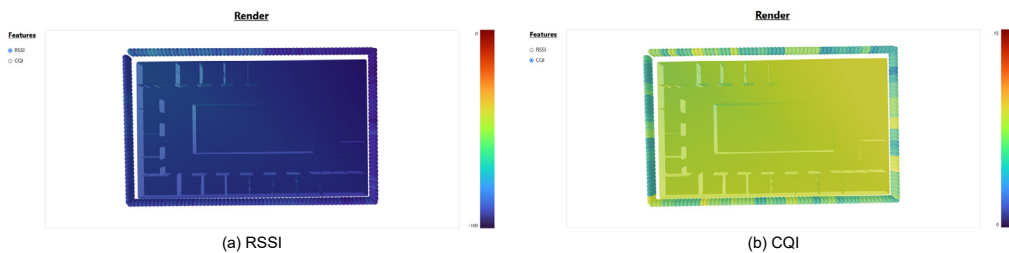


Fig. 7. In-building model reference points for (a) CQI and (b) RSSI

### 6.4. Validation of the proposed LA-DNN model

The proposed LA-DNN model was validated using walk-test in-building datasets, which served as ground truth data not used during model training. This process confirmed the model's predictive accuracy and reliability in estimating in-building coverage (IBC) signal metrics. Specifically, the model achieved an accuracy of 95.67% with a Root Mean Square Error (RMSE) of 8.75 dBm for Received Signal Strength Indicator (RSSI), and an accuracy of 97.13% with an RMSE of 2.08 for Channel Quality Indicator (CQI). Histogram visualizations illustrated a strong alignment between predicted and actual distributions, underscoring the model's effectiveness in accurately estimating both RSSI and CQI. These results affirm the framework's reliability and scalability for practical real-world deployment. Figure 8 presents a comparative analysis of the model's predictions against actual indoor measurements. For CQI (Fig. 8(a)), the predicted values closely align with actual measurements, with minor discrepancies observed in the range of 6–12, indicating reliable performance with occasional deviations. For RSSI (Fig. 8(b)), predictions exhibit tighter clustering, particularly between -110 and -70 dBm, demonstrating higher accuracy and stability.

Prediction error heatmaps for CQI (Fig. 8(c)) and RSSI (Fig. 8(d)) highlight the differences between predicted and actual values. RSSI errors are lower and more consistent, with occasional spikes at extreme

values (e.g.,  $\text{RSSI}_{\text{int}} = -65$  dBm). In contrast, CQI errors show greater variability, with notable inaccuracies at specific values (e.g.,  $\text{CQI}_{\text{int}} = 11, 8, 6$ ). These findings reflect the inherent complexity of CQI prediction, influenced by factors such as modulation and channel conditions, suggesting that further refinement in feature engineering could enhance model performance in these areas.

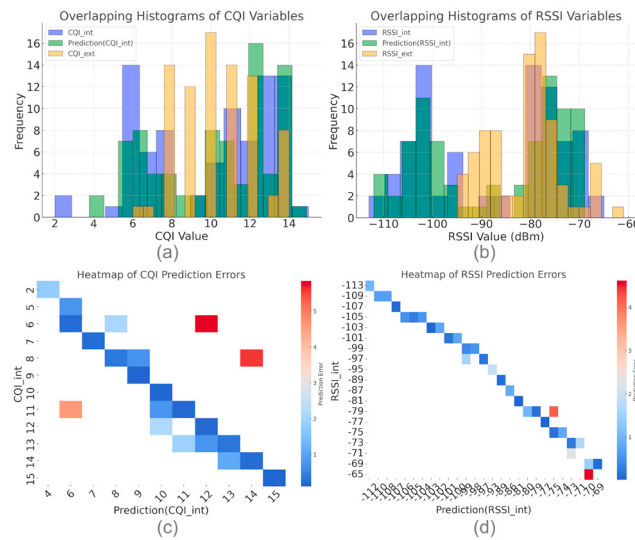


Fig. 8. Validation of the proposed LA-DNN model against real indoor measurements: (a) CQI and (b) RSSI overlapping histograms; (c) CQI and (d) RSSI prediction error heatmaps. The results demonstrate lower and more consistent errors for RSSI compared to greater variability in CQI predictions.

## 7. Discussion and Conclusion

This study demonstrates the feasibility and efficiency of integrating unmanned aerial vehicle (UAV)-based radio frequency (RF) data collection with a Location-Aware Deep Neural Network (LA-DNN) to predict in-building 5G signal coverage. By employing drones for external RF data acquisition, this approach substantially reduces the time and cost associated with traditional indoor walk tests. The LA-DNN, trained on external measurements enriched with spatial and material-specific features, accurately predicts complex signal distributions within high-rise buildings—a critical advancement for planning and optimizing indoor network infrastructure. The incorporation of 3D heatmaps enhances the interpretability of these predictions, allowing network engineers to identify coverage gaps and RF null zones with precision, thereby enabling targeted optimization strategies. The methodology effectively combines traditional in-building coverage (IBC) prediction techniques with data-driven models. By leveraging machine learning to model indoor coverage from externally captured 5G signal parameters, the framework provides a scalable, cost-effective solution while maintaining high prediction accuracy. The model excels at predicting 5G signal coverage in buildings with reinforced concrete core structures, as validated in this study. It could potentially adapt to other core types, such as traditional steel or composite frames, by incorporating material-specific RF propagation characteristics into the training data. However, its reliance on external data may limit applicability in scenarios where building structural details are unavailable or drone operations are restricted. While these features provide a strong foundation for adaptability, the model's performance across an extensive spectrum of architectural complexities (e.g., highly irregular floor plans or buildings constructed with unique materials not extensively represented in the training data) would benefit from further large-scale validation. Future work could explore real-time data integration, refined deep learning architectures, and validation across varied building materials and layouts to address these constraints and further enhance the framework's scalability and practical utility.

## Acknowledgements

This work is partially supported by the Australian Research Council under grant number: DP22010371, LE220100078, DP200101374 and LP170100891.

## References

- [1] Chandra, K., Prasad, R. V., Quang, B., Niemegeers, I. G. M. M. (2015). CogCell: cognitive interplay between 60 GHz picocells and 2.4/5 GHz hotspots in the 5G era. *IEEE Communications Magazine*, 53(7), 118–125.
- [2] Tsavdaridis, K. D., Nicolaou, A., Mistry, A. D., Efthymiou, E. (2020). Topology optimisation of lattice telecommunication tower and performance-based design considering wind and ice loads. *Structures*, 27, 2379–2399.
- [3] Asp, A., Sydorov, Y., Valkama, M., Niemelä, J. (2012). Radio signal propagation and attenuation measurements for modern residential buildings. *2012 IEEE Globecom Workshops*, 580–584.
- [4] Wang, C.-X., Haider, F., Gao, X., You, X.-H., Yang, Y., Yuan, D., Aggoune, H. M., Haas, H., Fletcher, S., Hepsaydir, E. (2014). Cellular architecture and key technologies for 5G wireless communication networks. *IEEE Communications Magazine*, 52(2), 122–130.
- [5] Ghanem, K., Alradwan, H., Motermawy, A., Ahmad, A. (2012). Reducing ping-pong Handover effects in intra EUTRA networks. *2012 8th International Symposium on Communication Systems, Networks Digital Signal Processing (CSNDSP)*, 1–5.
- [6] Fotouhi, A., Qiang, H., Ding, M., Hassan, M., Giordano, L. G., Garcia-Rodriguez, A., Yuan, J. (2019). Survey on UAV cellular communications: Practical aspects, standardization advancements, regulation, and security challenges. *IEEE Communications Surveys Tutorials*, 21(4), 3417–3442.
- [7] Kong, L., Tan, J., Huang, J., Chen, G., Wang, S., Jin, X., Zeng, P., Khan, M., Das, S. K. (2022). Edge-computing-driven internet of things: A survey. *ACM Computing Surveys*, 55(8), 1–41.
- [8] Ahmed, G., Sheltami, T., Ghaleb, M., Hamdan, M., Mahmoud, A., Yasar, A. (2024). Energy-Efficient Internet of Drones Path-Planning Study Using Meta-Heuristic Algorithms. *Applied Sciences*, 14(6), 2418.
- [9] Ouamri, M. A., Oteşteanu, M.-E., Barb, G., Gueguen, C. (2022). Coverage analysis and efficient placement of drone-BSs in 5G networks. *Engineering Proceedings*, 14(1), 18.
- [10] Tarekegn, G. B., Juang, R.-T., Lin, H.-P., Munaye, Y. Y., Wang, L.-C., Bitew, M. A. (2022). Deep-reinforcement-learning-based drone base station deployment for wireless communication services. *IEEE Internet of Things Journal*, 9(21), 21899–21915.
- [11] Yuliana, H., others. (2024). Comparative Analysis of Machine Learning Algorithms for 5G Coverage Prediction: Identification of Dominant Feature Parameters and Prediction Accuracy. *IEEE Access*.
- [12] Davies, J. N., Grout, V., Picking, R. (2008). Prediction of Wireless Network Signal Strength Within a Building. *INC*, 193–207.
- [13] Friis, H. T. (1946). A note on a simple transmission formula. *Proceedings of the IRE*, 34(5), 254–256.
- [14] Alsamhi, S. H., Almalki, F. A., Ma, O., Ansari, M. S., Lee, B. (2021). Predictive estimation of optimal signal strength from drones over IoT frameworks in smart cities. *IEEE Transactions on Mobile Computing*, 22(1), 402–416.
- [15] Behjati, M., Zulkifley, M. A., Alobaidy, H. A. H., Nordin, R., Abdullah, N. F. (2022). Reliable aerial mobile communications with RSRP RSRQ prediction models for the Internet of Drones: A machine learning approach. *Sensors*, 22(15), 5522.
- [16] Khoshkholgh, M. G., Navaie, K., Yanikomeroğlu, H., Leung, V. C. M., Shin, K. G. (2019). Coverage performance of aerial-terrestrial HetNets. *2019 IEEE 89th Vehicular Technology Conference (VTC2019-Spring)*, 1–5.
- [17] Cui, J., Hu, B., Chen, S. (2021). A decision-making scheme for UAV maximizes coverage of emergency indoor and outdoor users. *Ad Hoc Networks*, 112, 102391.
- [18] Kolawole, O., Hunukumbure, M. (2022). A drone-based 3D localization solution for emergency services. *ICC 2022-IEEE International Conference on Communications*, 1–6.
- [19] Dhokne, A., Gowda, M., Choudhury, R. R. (2017). Extending cell tower coverage through drones. *Proceedings of the 18th International Workshop on Mobile Computing Systems and Applications*, 7–12.
- [20] Infovista. (2025). Indoor and drone-based network testing and troubleshooting TEMS Pocket v26.0. <https://www.infovista.com>, 1–12.
- [21] Mikaelz. (2025). map-gmon-wifi-data v1.0. <https://github.com/mikaelz/map-gmon-wifi-data>, 1–12.
- [22] Sullivan, C., Kaszynski, A. (2019). PyVista: 3D plotting and mesh analysis through a streamlined interface for the Visualization Toolkit (VTK). *Journal of Open Source Software*, 4(37), 1450.
- [23] Otsu, N., others. (1975). A threshold selection method from gray-level histograms. *Automatica*, 11(285-296), 23–27.
- [24] Canny, J. (1986). A computational approach to edge detection. *IEEE Transactions on Pattern Analysis and Machine Intelligence*, 6(6), 679–698.
- [25] Galamhos, C., Matas, J., Kittler, J. (1999). Progressive probabilistic Hough transform for line detection. *Proceedings. 1999 IEEE Computer Society Conference on Computer Vision and Pattern Recognition*, 1, 554–560.
- [26] Raj, N. (2021). Indoor RSSI prediction using machine learning for wireless networks. *2021 International Conference on Communication Systems NETWORKS (COMSNETS)*, 372–374.